Volume 2
Number 4
July 2025
Pages 491–618

RSC Mechanochemistry

rsc.li/RSCMechanochem

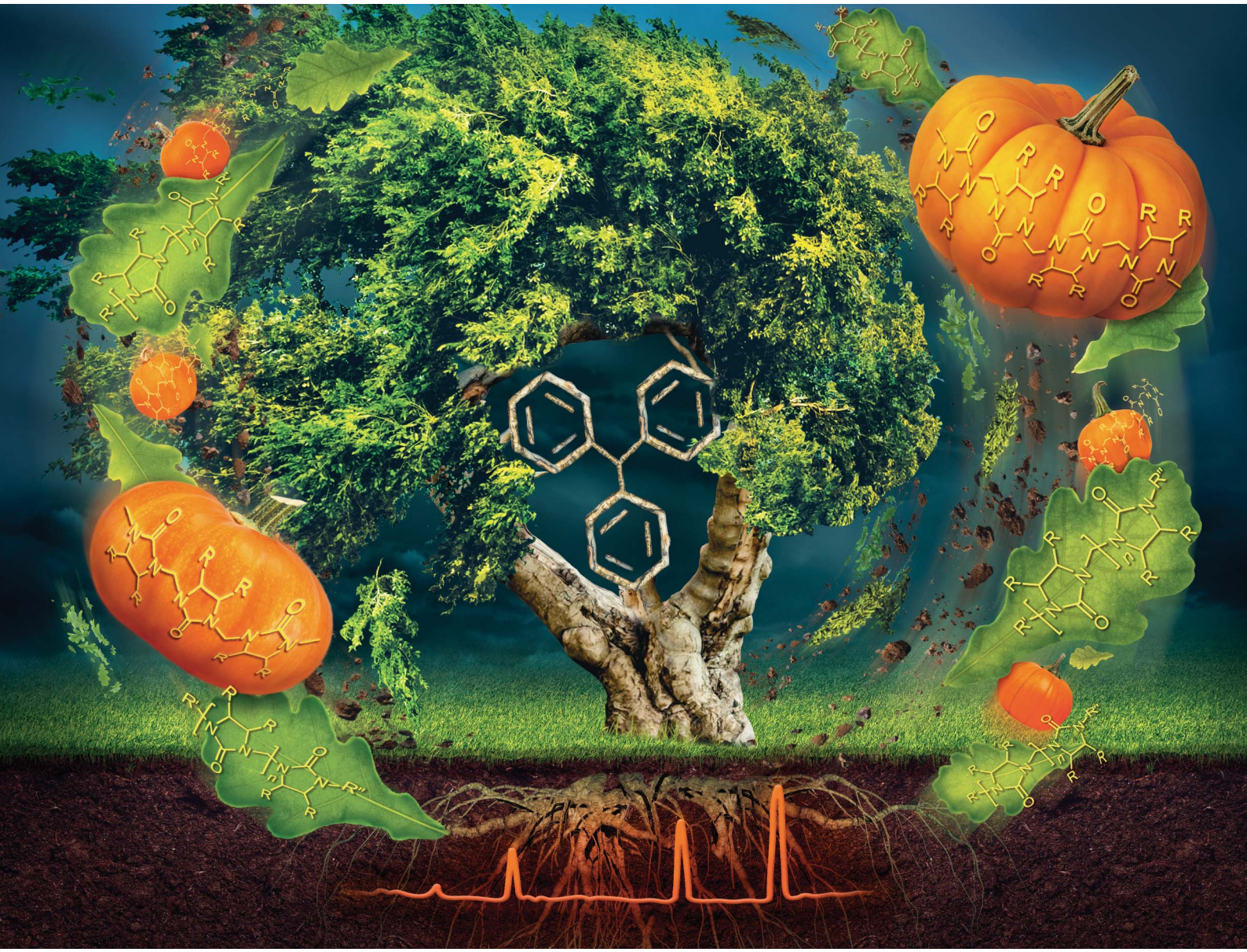

ISSN 2976-8683

ROYAL SOCIETY OF CHEMISTRY

PAPER

Riina Aav *et al.*

How reliable is internal standard method in monitoring mechanochemical synthesis? A case study of triphenylmethane in HPLC-UV-MS analysis of hemicucurbit[*n*]urils

RSC Mechanochemistry

ROYAL SOCIETY OF CHEMISTRY

PAPER

View Article Online
View Journal | View Issue

Cite this: *RSC Mechanochem.*, 2025, **2**, 507

How reliable is internal standard method in monitoring mechanochemical synthesis? A case study of triphenylmethane in HPLC-UV-MS analysis of hemicucurbit[*n*]urils†

Tatsiana Jarg, Jevgenija Tamm, Elina Suut-Tuule, Ketren-Marlein Lootus, Dzmitry Kananovich and Riina Aav *

Quantitative analysis of crude reaction mixtures is essential for the development of new synthetic methodologies and conducting mechanistic studies. While internal standard method is widely used for determining reaction yields in homogeneous solvent-based organic synthesis, its application in mechanochemical synthesis, which often involves heterogeneous mixtures, has not been properly validated. This study showcases applicability of triphenylmethane (TPM) as a solid internal standard in liquid-assisted, multi-component synthesis of homomeric cycHC[8] and mono-biotinylated mixHC[8] eight-membered cyclohexanohemicucurbit[*n*]urils. A fast and reliable HPLC-UV-MS analytical procedure was developed to determine yields by analyzing crude reaction mixtures, as a prerequisite of applying design-of-experiments optimisation approach. The influence of various parameters, including TPM concentration, reactant mixture weight, milling time, and the type and amount of liquid-assisted grinding additive, on the validity of the analysis was systematically studied. The results indicate that the primary challenge to trustworthy analysis arises from the non-uniform distribution of components. However, this issue can be detected with proper sampling and mitigated by optimising parameters to ensure uniform distribution of the internal standard throughout the reaction mixture. The results could be valuable for ensuring the credibility of *ex situ* and *in situ* analytical methods used to track the progress of mechanochemical reactions through single-point measurements.

Received 20th December 2024
Accepted 6th April 2025

DOI: 10.1039/d4mr00145a

rsc.li/RSCMechanochem

Introduction

Mechanochemical organic synthesis is gaining attention as a greener and more environmentally benign alternative to traditional synthesis in organic solvents.[1–3] Additionally, it enhances the reactivity of solids, leading to faster, higher-yielding, and more selective chemical reactions.[4,5] These benefits have led to the emergence and rapid growth of new advanced synthetic methods that rely on mechanochemical activation,[6,7] as well as a significant increase in their applications, including the synthesis of complex molecules such as pharmaceuticals,[8–13] functional materials,[14–17] supramolecules[18,19] and macrocyclic cavitands.[20–31] The development, optimisation, kinetic tracking, and mechanistic studies of mechanochemical reactions require a robust, widely accessible, and convenient analytical method for the rapid and reliable determination of product yields in the crude reaction mixtures. This is especially important when applying the design-of-experiments approach for rational screening and optimisation,[32] which is also a prerequisite for automation in future.[33]

Mechanochemical reactions can be conveniently monitored *in situ*[34,35] by powder X-ray diffraction (PXRD),[36] Raman,[37] X-ray absorption[38] and solid-state nuclear magnetic resonance (NMR)[39,40] spectroscopy, which provide valuable information on reactivity and real-time kinetics without interrupting the process. Quantitative PXRD monitoring with the addition of crystalline silicon, which addresses the issue of sample amount variation within the vessel, is a rare example of using the internal standard method for *in situ* analysis of mechanochemical reactions.[41]

However, the progress of mechanochemical reactions is prevalently followed by more accessible *ex situ* monitoring methods, such as NMR,[8,10,12,20–22,26,42] Fourier-transform infrared (FTIR)[8,20,24] and UV-vis[23,25,42] spectroscopies. While the application of these techniques is straightforward for analysing reactions that produce a single major component, reactions that yield complex mixtures may require additional chromatographic separation. For instance, high-performance liquid chromatography coupled with mass spectrometry (HPLC-MS) has been used for analysis of challenging systems.[13,26–28,30,31]

Department of Chemistry and Biotechnology, Tallinn University of Technology, Akadeemia tee 15, 12618 Tallinn, Estonia. E-mail: riina.aav@taltech.ee

† Electronic supplementary information (ESI) available. See DOI: https://doi.org/10.1039/d4mr00145a

In traditional solvent-based organic synthesis, an internal standard is often employed for quantitative analysis, typically using ^{1}H NMR spectroscopy.[43,44] The selection of the internal standard must meet certain criteria: it should be non-volatile, chemically inert, and uniformly distributed within the reaction medium. While uniform distribution is easily achieved in organic solvents, it is not guaranteed under mechanochemical conditions, where inhomogeneity and fluctuating multi-phase compositions are common. The effectiveness of mass transfer in these systems depends on the nature of the compounds as well as specific factors such as milling frequency and duration, the number and size of milling balls, the presence of liquid-assisted grinding (LAG) additives, and the degree of jar filling.[5] Although the issue of potential non-uniform distribution of the internal standard can be mitigated by homogenizing the entire reaction mixture during work-up, concerns about the reliability of the internal standard method remain when single-point sampling is involved. This challenge is particularly relevant in upscaled preparations and scenarios where samples are collected from the reaction mixture at regular intervals. In such cases, the trustworthiness of the method may be compromised. Additionally, some reactants, LAG additives, and products may be volatile, potentially altering the total mass of the reaction mixture and leading to inaccurate yield calculations. To the best of our knowledge, there have been no systematic studies validating the internal standard method in mechanochemistry for this type of measurements.

Here, we present a case study demonstrating the successful use of triphenylmethane (TPM) as a solid internal standard for the reliable determination of macrocyclic product yields from crude reaction mixtures (Fig. 1) obtained through a dynamic covalent chemistry approach. Cyclohexanohemicucurbit[*n*]urils (cycHC[*n*], $n = 6$ or 8) are the first examples of hemicucurbit[*n*]uril macrocycles[45] synthesized both in solution[46,47] and mechanochemically *via* ball-milling.[26] These cavitands form in a stepwise process, first producing linear oligomers by polycondensation of urea monomers with formaldehyde, followed by cyclisation of the oligomeric chains around a suitable anionic template. Thermodynamic equilibrium is reached during the aging of the reaction mixture at elevated temperatures, which enhances templation during macrocyclisation in the solid state.[26,31] Both steps are reversible and generate a diverse array of intermediates, resulting in a dynamic covalent library (DCL).[48] The number of produced species rapidly increases when distinct urea monomers are used, such as in the assembly of mono-biotinylated cyclohexanohemicucurbit[8]uril (mixHC[8]).[31] Additionally, the acid-catalysed condensation of urea monomers with formaldehyde produces water, leading to a fluctuating liquid-to-solid ratio (η, µl mg^{-1})[49] at the milling and aging stages, and sample preparation. In the synthesis of mixHC[8], the content of water resulting from LAG additive and condensation can make up to approximately 20% of reaction mixture by weight. The varying multi-phase, multi-component composition of the reaction mixture and the risks of uncontrollable water evaporation during aging at elevated temperatures pose significant challenges for analysis. We discovered that quantitative HPLC-UV-MS is more advantageous for analysing the DCL complexity compared to PXRD, FTIR, and NMR.

During the optimisation of the synthesis, we gathered a large dataset from over 100 reaction runs, which enabled us to pinpoint the conditions under which the internal standard method yields reliable results, as well as to identify conditions that could lead to erroneous single-point measurements due to non-uniform distribution of the internal standard. The reliability of the method was evaluated through assessments of stability, linearity, limits of detection (LoD) and quantitation (LoQ), accuracy, and reproducibility.

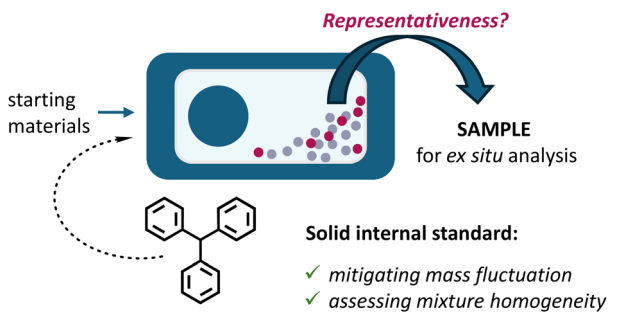

Fig. 1 Addition of a solid internal standard prior to milling to improve the representativeness of single-point samples for *ex situ* analysis, investigated in this work.

Experimental

Materials, reagents and solvents

All reagents were purchased from commercial suppliers. HPLC grade solvents (acetonitrile, isopropanol, absolute ethanol, chloroform stabilized with amylene) and LC-MS grade formic acid were procured from Thermo Fischer Scientific. The cycHC[*n*] used as the reference standards were synthesized in our laboratory according to the published procedures.[26,46,47] The purity of the macrocycles (90–98%) was determined by quantitative ^{1}H NMR.[50]

Mechanochemical synthesis of mixHC[8]

D-Biotin (46 mg, 0.19 mmol, 1 equiv.), (*R*,*R*)- or (*S*,*S*)-*N*,*N*′-cyclohexa-1,2-diylurea (183 mg, 1.30 mmol, 7 equiv.), paraformaldehyde (45 mg, 1.50 mmol, 8 equiv.) and triphenylmethane (5–15 mg, as internal standard for HPLC yield determination) were placed into a 14 mL ZrO_2 jar sleeved in aluminium and charged with two 10 mm ZrO_2 balls (*ca.* 3.5 g). The template and LAG additive consisting of aqueous acid or acid combined with the corresponding salt (0.56 mmol, 3 equiv.) was added to the mixture, which was then set to mill in a Form-Tech Scientific FTS-1000 shaker mill at 30 Hz for 1 h. Subsequently, the milling jar was sealed with parafilm and reaction mixture was aged in a VWR INCU-Line IL10 incubator at 60 °C for 24 h, and the resulting crude mixture was quenched with water and dried under air at room temperature. The sampling for HPLC-UV-MS analysis was performed after the aging step, before quenching; the amounts of starting materials

and reagents, as well as milling time and aging temperature varied during screening and optimisation experiments.[31]

PXRD

PXRD analysis was performed on Bruker D8 Advanced Diffractometer with Fe-filtered Co radiation and LynxEye detector, collecting data in the range of 2θ from 4 to 40°. The samples (*ca.* 38 mg) were mixed with absolute ethanol (2–3 drops) to form a paste, which was spread on a glass slide.

FTIR spectroscopy

The vibrational spectra were recorded on Bruker Tensor 27 FTIR spectrometer. The samples were prepared as KBr pellets (*ca.* 1.7 mg crude reaction mixture and *ca.* 125 mg KBr).

^{1}H NMR spectroscopy

^{1}H NMR spectra were acquired on 400 MHz Bruker Avance III spectrometer. The samples were prepared by dissolving *ca.* 20 mg of reaction mixture in 1 : 1 mixture of perdeuterated chloroform and methanol. All chemical shifts were reported in ppm units and referenced to tetramethylsilane (δ ^{1}H 0.00 ppm).

HPLC-UV-MS

HPLC-UV-MS analysis was carried out on Agilent 1200 Series System, comprising a G1322A degasser, low-pressure mixing G1311A quaternary pump, G1329A autosampler, G1316A thermostated column compartment, G1365B multi-wavelength detector, and a G6125B single quadrupole mass detector (mass accuracy ±0.13 Da) equipped with a multimode ion source. The chromatographic separation was performed on a Phenomenex Kinetex XB-C18 column (150 mm × 4.6 mm, 2.6 μm). Eluents A (water/0.1% formic acid) and B (acetonitrile/0.1% formic acid) were used in a 10-minute gradient from A : B 50 : 50 (v/v) to A : B 10 : 90 (v/v), followed by a 2-minute isocratic hold at A : B 10 : 90 (v/v). The composition then returned to A : B 50 : 50 (v/v) over 1 minute, with a 4-minute equilibration step. The flow rate was maintained at 0.75 mL min^{-1}. The column temperature was set at 30 °C and injection volume at 2 μL. UV-absorbance was monitored at 210 nm detection wavelength with a 4 nm bandwidth without a reference, using a standard 10 mm, 13 μL flowcell. The peaks were identified by electrospray ionisation mass spectrometry (ESI-MS) with the following spray chamber parameters: drying gas flow 5 L min^{-1}, drying gas temperature 300 °C, nebulizer pressure 60 psig, vaporizer temperature 150 °C, capillary voltage 2000 V and charging electrode voltage 2000 V. The mass spectra were acquired in positive ionisation mode within m/z 500–2000 range and fragmentor voltage 80 V.

Sample preparation

The crude reaction mixture (*ca.* 300 mg) distributed across the surface of the jar and milling balls was combined using a spatula, and random sampling was performed from different sections of the reaction vessel, providing minimum three *ca.* 1 mg probes. Each probe was dissolved in chloroform : isopropanol 1 : 1 (v/v) mixture to prepare a sample with a concentration *ca.* 1 mg mL^{-1}. The solution was then filtered through 0.2 μm PTFE membrane syringe filter to remove salt templates insoluble in organic solvents.

Calibration procedure

Stock solutions of mixHC[8], cycHC[8], cycHC[6] and TPM were prepared using Radwag MYA 11.4Y microbalances and calibrated automatic pipettes of 20–200 μL and 100–1000 μL volumes. Calibration solutions of known concentrations were prepared in three parallels by consequent dilution of three independent stock solutions, using chloroform : isopropanol 1 : 1 (v/v) mixture as the solvent. The concentration range varied from 0.9 mg mL^{-1} to LoD (see ESI† for more details).

The calibration graphs were constructed by plotting peak areas against the concentration. The obtained ten-point calibration curves for each compound were fitted using linear regression analysis, yielding linear equations ($y = kx$, with the intercept was set to 0) and corresponding R^2 values.

Determination of yields

The macrocyclic content was quantified *via* calibration graphs. The conversion of starting materials to products was determined as the ratio of urea monomers incorporated into the macrocycle (*i.e.*, the amount of macrocycle multiplied by the number of monomeric units) to the total monomer content, and expressed as the macrocycle yield. Formulae (1)–(6) were used to derive the final eqn (7) used for yield calculation:

$$\%\ \text{Yield} = \frac{n_{\text{HC}} \cdot N_{\text{mon}}}{n_{\text{st.mon}}} \times 100 \tag{1}$$

$$n_{\text{HC}} = \frac{m_{\text{RM}} \cdot \omega_{\text{HC,RM}}}{M_{\text{HC}}} \tag{2}$$

$$\omega_{\text{HC,RM}} = \omega_{\text{HC,CMA}} \cdot f = \frac{\omega_{\text{HC,CMA}} \cdot \omega_{\text{IS,RM}}}{\omega_{\text{IS,CMA}}} \tag{3}$$

$$\omega_{\text{HC,CMA}} = \omega_{\text{HC,S}} = \frac{c_{\text{HC}}}{c_{\text{S}}} = \frac{S_{\text{HC}} \cdot V_{\text{S}}}{k_{\text{HC}} \cdot m_{\text{S}}} \tag{4}$$

$$\omega_{\text{IS,CMA}} = \omega_{\text{IS,S}} = \frac{c_{\text{IS}}}{c_{\text{S}}} = \frac{S_{\text{IS}} \cdot V_{\text{S}}}{k_{\text{IS}} \cdot m_{\text{S}}} \tag{5}$$

$$\omega_{\text{IS,RM}} = \frac{m_{\text{IS}} \cdot P_{\text{IS}}}{m_{\text{RM}} \times 100} \tag{6}$$

$$\%\ \text{Yield} = \frac{S_{\text{HC}} \cdot k_{\text{IS}} \cdot m_{\text{IS}} \cdot P_{\text{IS}} \cdot N_{\text{mon}}}{S_{\text{IS}} \cdot k_{\text{HC}} \cdot M_{\text{HC}} \cdot n_{\text{st.mon}}} \tag{7}$$

where n_{HC} – the number of moles of the macrocycle, mmol; N_{mon} – number of monomeric units in the macrocycle; $n_{\text{st.mon}}$ – total number of moles of starting monomers (biotin and (*R*,*R*)-*N*,*N*′-cyclohexa-1,2-diylurea), mmol; m_{RM} – total mass of reactant mixture, including internal standard, mg; M_{HC} – molar weight of the macrocycle, g mol; $\omega_{\text{HC,RM}}$, $\omega_{\text{HC,CMA}}$ and $\omega_{\text{HC,S}}$ – theoretical mass fraction of the macrocycle relative to the reactant mixture (recalculated *via* internal standard), in the

crude mixture after aging and in the sample, respectively; $\omega_{IS,RM}$, $\omega_{IS,CMA}$ and $\omega_{IS,S}$ – mass fraction of the internal standard in the reactant mixture based on the weighed amount, in the crude mixture after aging and in the sample based on analysis; f – correction factor (the ratio of internal standard percentage in the reactant mixture to its percentage in the sample, which represents crude mixture after aging); c_S, c_{HC} and c_{IS} – concentrations of the crude mixture after aging, macrocycle and internal standard in the sample solution, respectively, mg mL; m_S – mass of the crude mixture after aging used in the sample preparation, mg; V_S – volume of the solvent mixture used in the sample preparation, mL; S_{HC} and S_{IS} – peak areas of the macrocycle and internal standard, respectively, mAU s; k_{HC} and k_{IS} – the slopes of the calibration curves for the macrocycle and internal standard, respectively, mAU s mL mg^{-1}; m_S – mass of aged crude mixture sample, mg; V_S – volume of solvent mixture used in the sample preparation, mL; m_{IS} – mass of internal standard, mg; P_{IS} – purity of internal standard, %. For more details, see ESI (Scheme S1).†

The analysis was performed in triplicate, and the HPLC yields were reported as the mean value ± standard deviation between parallel measurements.

Linearity, LoQ and LoD

Linearity was assessed based on the plots of residuals and LINEST analysis. LoQ and LoD were determined by signal-to-noise ratio (S/N) of 10 and 3, respectively.

Accuracy and reproducibility

The test solution of crude reaction mixture containing internal standard, was spiked with small additions of TPM and macrocycles. The method accuracy, which shows the closeness of the analysis result to the true value, was evaluated by recovery bias, which reflects the difference between experimentally found and theoretical concentration values (for more details, see ESI†). Method reproducibility was assessed for 2 × 9 independent samples collected from two crude reaction mixtures, based on relative standard deviation (RSD).

Results and discussion

Multi-component self-assembly of mixHC[8] in solid state leads to a particularly complex mixture containing two major products (mixHC[8] and cycHC[8]) along with numerous linear intermediates as well as other macrocyclic species[31] (Fig. 2). The crude reaction mixtures were analysed after milling and after aging by PXRD, FTIR and ^{1}H NMR methods. As reported previously,[26] PXRD technique was not applicable for *in situ* monitoring of mechanochemical synthesis of cycHC[n] due to amorphous nature of the reaction mixture and difficulties in maintaining the controlled reaction environment. *Ex situ* PXRD analysis of the starting materials used in mixHC[8] synthesis revealed some crystalline phases, nevertheless the milled crude mixture samples, as well as the aged product samples were amorphous, making this methodology not suitable for reaction monitoring (Fig. S1†). The application of other spectroscopic techniques, such as FTIR and UV spectroscopies, is also limited, as no significant changes appear between the vibrational spectra of starting monomers, intermediates and macrocycles (Fig. S2–S6†), and no characteristic UV bands occur upon the formation of different products.[50]

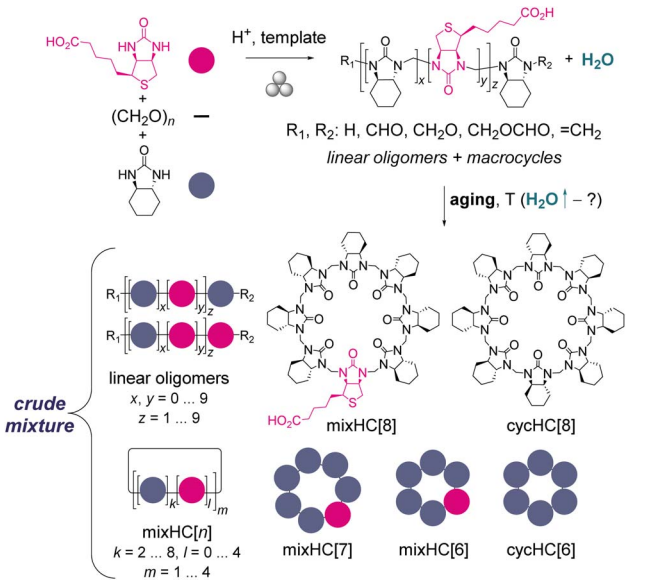

Fig. 2 General scheme of mixHC[8] synthesis in solid state, describing the composition of crude reaction mixture.

The large number of intermediates formed during the synthesis drastically complicate ^{1}H NMR spectra (Fig. S7–S11†), which undermines the application of conventional ^{1}H NMR for reliable data interpretation and quantitation. Therefore, employing a separation method, *e.g.* HPLC, appeared to be essential to ensure discrimination between the components. The individual analytes can be identified based on their retention times and using additional techniques such as MS.[26] In order to reliably determine yields, TPM was added as an inert solid internal standard to the mixture of reactants prior to milling. Importantly, the use of internal standard is advantageous since it allows to mitigate the problem of uncontrollable evaporation of water at the aging step and during subsequent manipulations with the sample.

Development of method for quantitative HPLC-UV analysis

Separation of mixHC[8] crude mixture components by HPLC-UV provided chromatograms suitable for quantification (Fig. 3A). ESI-MS analysis confirmed the formation of the two major macrocycles – mixHC[8] and cycHC[8], accompanied by minor by-products, found at trace levels under UV and MS detection: di-biotinylated mixHC[8], mixHC[7], mixHC[6], cycHC[6] (Fig. 3B, S12 and Table S1†). Generally, HPLC-UV chromatograms contained only peaks belonging to the macrocycles, as the linear oligomers have significantly lower UV-absorbance.[50]

The stability of sample solution was investigated in different solvent mixtures. The cycHC[n] macrocycles are most soluble in chlorinated solvents, such as chloroform, while biotin and biotin-containing oligomers prefer more polar solvents, such as

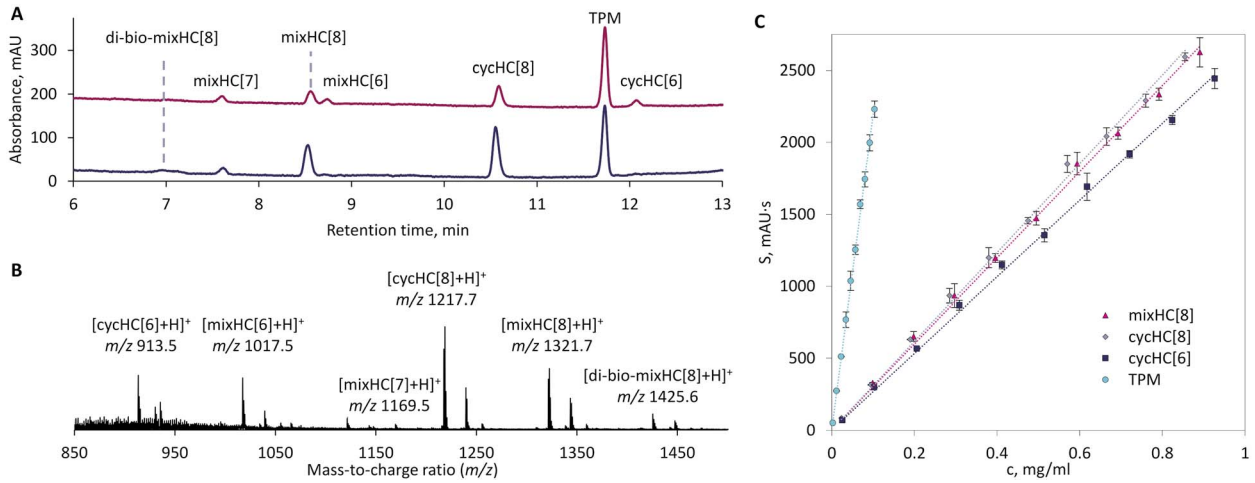

Fig. 3 (A) Representative HPLC-UV chromatograms of the crude reaction mixtures obtained in two separate experiments (detection at 210 nm); (B) (+)ESI-MS spectrum of the depicted chromatogram region used for peak identification; (C) calibration curves for determination of HPLC yields, the error bars represent standard deviation between triplicates.

methanol. Therefore, chloroform was mixed with an alcohol to ensure sample miscibility with an aqueous-based eluent. Since the mixHC[8] crude mixture contains strong mineral acid used in the synthesis ($HClO_4$ or HPF_6), the products and intermediates can still undergo dynamic interconversion in solution. Moreover, acidic medium initiates esterification[51] of biotin carboxylic group and affects sample stability. Esterification rate, however, depends on alcohol reactivity, for instance, isopropanol provides solutions stable for at least 24 h compared to methanol, where esterification occurs much faster (Table S2 and Fig. S13†).

Plotting peak areas against the corresponding concentrations of the macrocycles and internal standard confirmed linear dependency between their concentration and UV signal with correlation coefficients $R^2 > 0.995$ and random residuals throughout the range of method application (Fig. 3C, S14 and Table S3†). Previously reported quantitative HPLC-UV procedure described the UV-absorption properties of cycHC[n] homologues,[50] and based on the slopes of the calibration curves the new mono-biotinylated mixHC[8] exhibited a response nearly identical to that of cycHC[8]. Compared to the macrocycles, the TPM absorbance was found to be *ca.* 7 times stronger, which justifies using low amounts of internal standard. The developed HPLC-UV-MS method demonstrated sufficiently low LoQ and LoD, allowing for detection of minor macrocyclic products (*ca.* 1% w/w).

Distribution of internal standard during ball milling

TPM was selected as the internal standard due to its convenient solid form, prominent UV absorbance and chemical inertness under the reaction conditions. The latter was confirmed by ball milling of TPM and starting materials in the presence of HPF_6, resulting in (98.7 ± 0.5)% internal standard recovery upon analysis of the entire reaction mixture, which was quantitatively transferred into a 100 mL volumetric flask, dissolved in the solvent mixture and filtered (Fig. 4A and Table S4†).

However, the recovery values obtained *via* replicate triple-point sampling showed noticeable variation between different reaction runs and recovery bias values, mainly affected by the LAG additive and its nature (Fig. 4A and Table S4†). Neat grinding (NG) in the absence of acid prevented polycondensation and ensured permanent composition of solids upon mechanical mixing, resulting in (98.2 ± 0.4)% TPM recovery with low variation. The reaction with 60% aq. HPF_6

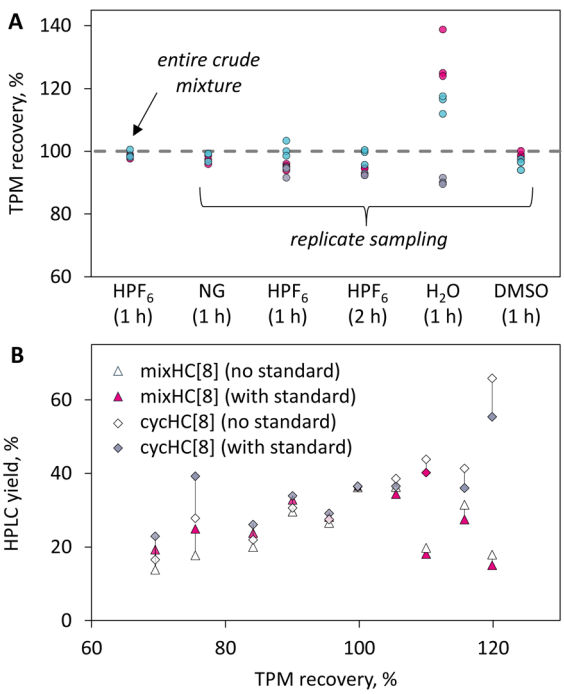

Fig. 4 (A) Recovery of the internal standard after ball milling 300 mg solids at 30 Hz under NG and LAG (60% aq. HPF_6, water or DMSO, $\eta = 0.2$ μL mg^{-1}) conditions; independent milling experiments are colour-coded, the points correspond to the replicate analyses; (B) the estimated error of yield determination using or neglecting the internal standard, indicated by filled and hollow markers, respectively.

provided (96 ± 4)% and (95 ± 3)% recoveries after 1 h and 2 h of milling, respectively, and noticeable variance between the parallels. The observed differences between reactions performed under identical conditions could point at the LAG effects on mixing efficiency. The experiment with addition of pure water instead of aqueous HPF_6 caused recovery bias up to 39% and large variation of the obtained TPM recovery values (112 ± 20)%. We hypothesised that the observed non-uniformity in the sample content could be caused by poor miscibility of hydrophobic internal standard and starting materials (except biotin) with water, that prevents proper homogenization during the milling. The latter was supported by replacing water with DMSO which can solubilize both the monomers and TPM. Indeed, DMSO as a LAG additive resulted in much better mixing and consequently smaller bias and variation of the recovery values (98 ± 2)%. In agreement with previous, the presence of aqueous acid induces protonation and higher polarity of solid surface, and therefore better mixing. However, the TPM recovery values observed during the yield determination of mixHC[8] and cycHC[8] macrocycles in the aged samples likely reflect uncontrollable water evaporation and absorption during milling, aging and sample preparation. In our study, these effects led to a change of up to 30% in the total mass of the reaction mixture (Fig. 4B). Consequently, the absence of an internal standard could produce misleading results.

The non-uniform distribution of the internal standard caused by inefficient mass transfer also results in erroneous analytical response. This prompted us to study how additional factors affect distribution of TPM in the reaction media. The explored variables included: (i) TPM loading (%, w/w), (ii) amount of LAG additive (60% aq. HPF_6, μL mg^{-1}), (iii) total mass of solid reactants and (iv) milling duration. Milling frequency (30 Hz) and number of balls (2 × 10 mm, *ca.* 3.5 g) were kept constant. Distribution of internal standard within the reaction mixtures was assessed based on relative standard deviation (RSD) of the TPM peak areas from the replicate measurements, RSD ≤ 5% was regarded as the acceptance criterion of sufficient homogeneity.

First, the data acquired from the reactions performed with variable amount of TPM (ranging from 1% to 4% w/w) showed no significant difference (RSD < 5%) in the distribution of the standard throughout the tested loading range (Fig. 5A and Table S5†). Second, the effect of the LAG agent loading was evaluated in the range of $\eta = 0.15–1.15$ μL mg^{-1} in 14 mL milling jars. As we showed before, the nature of LAG additive can cause adverse effects depending on the miscibility of LAG agent with solid components. In the case of mixHC[8] synthesis,[31] aqueous mineral acid, used as the catalyst and LAG additive, resulted in acceptably uniform distribution of the internal standard (RSD < 5%) at η < 0.5 μL mg^{-1} (Fig. 5B). However, higher η values resulted in increased inhomogeneity (RSD up to 10%, Fig. 5B and Table S6†). Third, the variable loading of the solids (range 280–390 mg) in 14 mL jar at η < 0.5 μl mg^{-1} kept distribution of the standard within the acceptable range(Fig. 5C, S15 and Table S6†). Finally, since mixing of solid reactants in mechanochemistry is time-dependent, the duration of milling was tested. Screening the milling times from 5 to 90 min resulted in uniform distribution of the internal standard in the aged mixtures (RSD < 5%, Fig. 5D and Table S7†), showing that homogeneity was achieved in rather short period of time. Overall, these results evidence that the nature of LAG agent and its loading have the most pronounced effect on the distribution of TMP among all studied parameters.

Distribution of products during ball milling

The distribution of the macrocyclic products in the crude mixtures followed the same trends observed for the internal standard (Fig. S16†), indicating that higher amount of LAG additive caused noticeable inhomogeneity. In such instances random replicate sampling from different points of the crude mixture is vital to increase reliability of the analysis. In addition, the data acquired during optimisation and screening experiments demonstrated that the distribution of the products is largely governed by the reaction outcome. Thus, ball-milling and aging performed under unfavourable conditions during optimisation in some cases resulted in poor yields, and

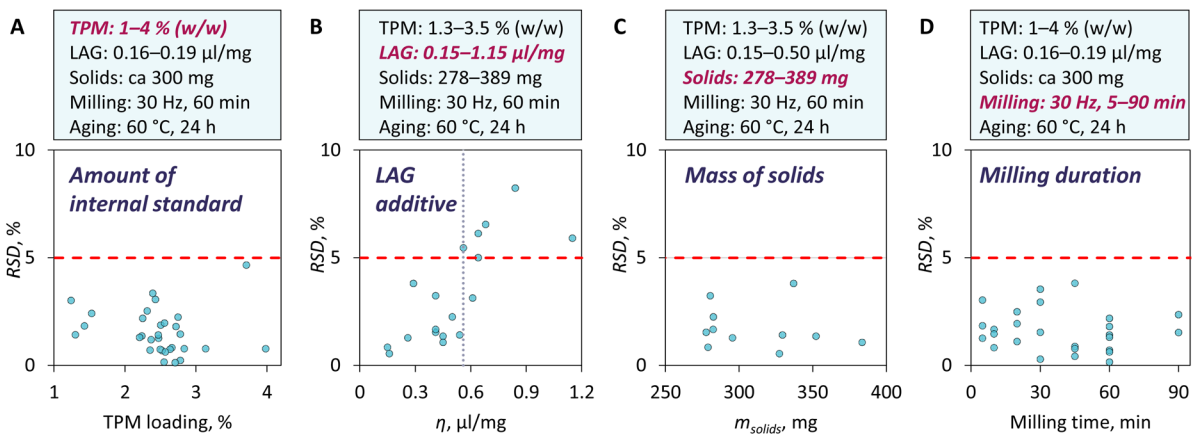

Fig. 5 Distribution of the internal standard across reaction mixture during milling depending on its concentration (A), LAG additive amount (B), mass of solid reactants (C) and milling duration (D), expressed as RSD of TPM peak areas acquired in triplicate measurements.

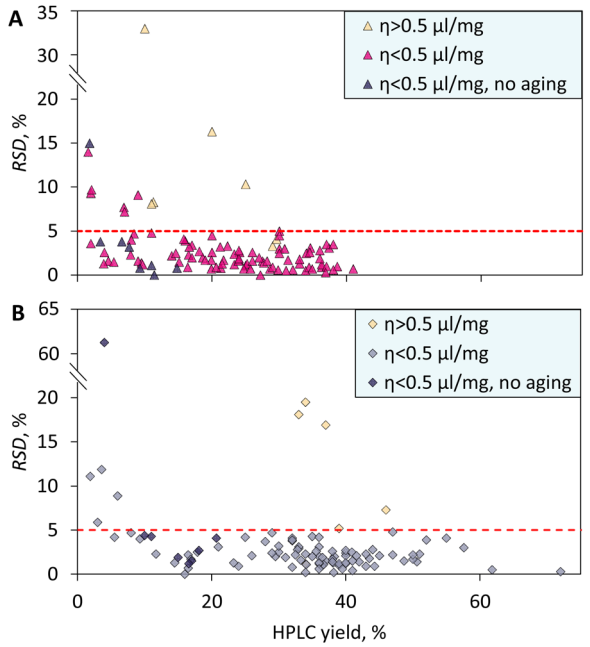

Fig. 6 Distribution of mixHC[8] (A) and cycHC[8] (B) in the crude mixtures under different reaction conditions, expressed as RSD of corresponding peak areas from replicate measurements (n = 3). For more details see Table S8.†

consequently higher variation of the replicate measurements (Fig. 6 and Table S8†).

The analysis of reactions carried out under optimal conditions prior to the aging step showcased the importance of the milling duration: the mixture milled for just 5 min afforded macrocycles in low yields with RSD values of 33% and 61% for mixHC[8] and cycHC[8], respectively (Fig. 6 and Table S8†). Noteworthy, the concentration of the internal standard was sufficiently uniform in all crude mixtures, with the exception of reactions with $\eta > 0.5$ μl mg^{-1} (Table S8†). These results show, that although 5 min mixing in a shaker mill was enough for the uniform distribution of the internal standard as a minor additive, it was not sufficient to homogenise other components of the mixture, which resulted in high RSD of yields across the reaction mixture. Therefore, analysing crude mixtures milled for a short period of time requires extra caution. Increasing the number of sampled probes can provide more reliable results.

Method accuracy was assessed based on spike recovery for TPM, mixHC[8] and cycHC[8] additions (Tables S9 and S10†). The bias did not exceed 2.7%, which was considered acceptable for the purpose of the current analysis.

Reproducibility studies were performed on two crude mixtures ball-milled and aged under optimal conditions *via* sampling 9 random probes from each vessel. The analysis resulted in *ca.* 1% standard deviation of the obtained yield values: (31 ± 1)% and (32 ± 1)% for mixHC[8] and cycHC[8], respectively. The RSD (n = 9) of the HPLC yield values satisfied the established 5% threshold (Table S11†). The variance of replicate measurements did not depend on additional mixing of the milling jar contents with a spatula prior to sampling.

Conclusions

In this study, we validated the use of TPM as an internal standard for determining yields in the mechanochemical synthesis of cyclohexanohemicucurbit[n]urils from a mixture of different urea monomers. This complex multicomponent reaction is characterised by the generation of numerous, interconvertible intermediates and products, the presence of an aqueous-based LAG additive poorly miscible with the starting materials, and a fluctuating liquid-to-solid ratio due to volatility of water. These factors pose significant challenges for chemical analysis, necessitating an efficient separation technique coupled with an internal standard for reliable yield determination.

To address these challenges, we developed a quantitative HPLC-UV-MS method using TPM as a solid internal standard to determine the yields of macrocyclic products from crude reaction mixtures. This method was further applied to optimise reaction conditions through a design-of-experiments approach.[31] The reliability of the method was confirmed through assessments of its linearity, accuracy, and reproducibility.

Importantly, we identified limitations in the internal standard methodology that could lead to erroneous yield values. These errors arose from the non-uniform distribution of the hydrophobic internal standard in the presence of an aqueous-based LAG agent. Our findings underscore the need to consider the miscibility of the internal standard with the LAG additive as a key selection criterion and highlight the importance of validating internal standard selection by ensuring its homogeneous distribution across the reaction mixture. In addition to reactions mediated by liquids, the solid internal standard approach may be utilized to access homogeneity of reaction mixtures performed under neat grinding conditions.

On the other hand, we found that the distribution of the internal standard was uniform (RSD < 5%) and was not significantly affected by its loading (1–4% w/w), the total mass of solids in the milling jars (280–390 mg), or the milling time (5–90 min). The macrocyclic products generally exhibited similar distribution trends to those of the internal standard, although reactions with low yields showed uneven product concentrations throughout the reaction vessel.

Given the potential for significant variability in component distribution depending on the reaction, any analytical method involving single-point measurements should be rigorously validated under mechanochemical conditions to ensure the credibility of the results. Uniform distribution across the reaction mixture should be verified through random replicate sampling, particularly for rapid reactions (<5 min) and systems with poorly miscible reactants that can lead to non-uniform reaction mixtures. Further studies on the application of the internal standard method for quantitative description of various mechanochemical processes will enhance understanding in the field.

Data availability

All experimental and characterization data and detailed experimental procedures are available in the published article and ESI.†

Author contributions

TJ: investigation, measurements, data collection, methodology, validation, analysis of results, writing – original draft; JT, EST, KML: investigation, data collection; DK: methodological advice, conceptualization, writing – review and editing; RA: supervision, methodology, conceptualization, writing – review and editing.

Conflicts of interest

The authors declare no conflicts of interest.

Acknowledgements

The research was funded by Estonian Research Council grant PRG2169, and by the Ministry of Education and Research through Centre of Excellence in Circular Economy for Strategic Mineral and Carbon Resources (01.01.2024–31.12.2030, TK228).

References

1 S. L. James, C. J. Adams, C. Bolm, D. Braga, P. Collier, T. Friščić, F. Grepioni, K. D. M. Harris, G. Hyett, W. Jones, A. Krebs, J. Mack, L. Maini, A. G. Orpen, I. P. Parkin, W. C. Shearouse, J. W. Steed and D. C. Waddell, *Chem. Soc. Rev.*, 2012, **41**, 413–447.
2 T. Friščić, C. Mottillo and H. M. Titi, *Angew. Chem., Int. Ed.*, 2020, **59**, 1018–1029.
3 R. T. O'Neill and R. Boulatov, *Nat. Rev. Chem*, 2021, **5**, 148–167.
4 G. A. Bowmaker, *Chem. Commun.*, 2013, **49**, 334–348.
5 J. L. Howard, Q. Cao and D. L. Browne, *Chem. Sci.*, 2018, **9**, 3080–3094.
6 K. Kubota, Y. Pang, A. Miura and H. Ito, *Science*, 2019, **366**, 1500–1504.
7 C. Patel, E. André-Joyaux, J. A. Leitch, X. M. de Irujo-Labalde, F. Ibba, J. Struijs, M. A. Ellwanger, R. Paton, D. L. Browne, G. Pupo, S. Aldridge, M. A. Hayward and V. Gouverneur, *Science*, 2023, **381**, 302–306.
8 D. E. Crawford, A. Porcheddu, A. S. McCalmont, F. Delogu, S. L. James and E. Colacino, *ACS Sustain. Chem. Eng.*, 2020, **8**, 12230–12238.
9 F. Puccetti, S. Lukin, K. Užarević, E. Colacino, I. Halasz, C. Bolm and J. G. Hernández, *Chem.–Eur. J.*, 2022, **28**, e202104409.
10 J. Gómez-Carpintero, C. Cabrero, J. D. Sánchez, J. F. González and J. C. Menéndez, *Green Chem. Lett. Rev.*, 2022, **15**, 638–645.
11 M. Lavayssiere and F. Lamaty, *Chem. Commun.*, 2023, **59**, 3439–3442.
12 R. Geib, E. Colacino and L. Gremaud, *ChemSusChem*, 2024, **17**, e202301921.
13 T. Nikonovich, T. Jarg, J. Martõnova, A. Kudrjašov, D. Merzhyievskyi, M. Kudrjašova, F. Gallou, R. Aav and D. Kananovich, *RSC Mechanochem.*, 2024, **1**, 189–195.
14 L. P. Jameson and S. V. Dzyuba, *Beilstein J. Org. Chem.*, 2013, **9**, 786–790.
15 M. Pérez-Venegas, T. Arbeloa, J. Bañuelos, I. López-Arbeloa, N. E. Lozoya-Pérez, B. Franco, H. M. Mora-Montes, J. L. Belmonte-Vázquez, C. I. Bautista-Hernández, E. Peña-Cabrera and E. Juaristi, *Eur. J. Org Chem.*, 2021, **2021**, 253–265.
16 T. Stolar and K. Užarević, *CrystEngComm*, 2020, **22**, 4511–4525.
17 E. M. Lloyd, J. R. Vakil, Y. Yao, N. R. Sottos and S. L. Craig, *J. Am. Chem. Soc.*, 2023, **145**, 751–768.
18 T. Friščić, *Chem. Soc. Rev.*, 2012, **41**, 3493.
19 A. Bose and P. Mal, *Beilstein J. Org. Chem.*, 2019, **15**, 881–900.
20 B. Içli, N. Christinat, J. Tönnemann, C. Schüttler, R. Scopelliti and K. Severin, *J. Am. Chem. Soc.*, 2009, **131**, 3154–3155.
21 M. Pascu, A. Ruggi, R. Scopelliti and K. Severin, *Chem. Commun.*, 2013, **49**, 45–47.
22 H.-T. Xi, T. Zhao, X.-Q. Sun, C.-B. Miao, T. Zong and Q. Meng, *RSC Adv.*, 2013, **3**, 691–694.
23 H. Shy, P. Mackin, A. S. Orvieto, D. Gharbharan, G. R. Peterson, N. Bampos and T. D. Hamilton, *Faraday Discuss.*, 2014, **170**, 59–69.
24 Y. Yang, F. Bu, J. Liu, I. Shakir and Y. Xu, *Chem. Commun.*, 2017, **53**, 7481–7484.
25 Q. Su and T. D. Hamilton, *Beilstein J. Org. Chem.*, 2019, **15**, 1149–1153.
26 S. Kaabel, R. S. Stein, M. Fomitšenko, I. Järving, T. Friščić and R. Aav, *Angew. Chem., Int. Ed.*, 2019, **58**, 6230–6234.
27 E. Oliva, D. Mathiron, S. Rigaud, E. Monflier, E. Sevin, H. Bricout, S. Tilloy, F. Gosselet, L. Fenart, V. Bonnet, S. Pilard and F. Djedaini-Pilard, *Biomolecules*, 2020, **10**, 339.
28 T. Dalidovich, K. A. Mishra, T. Shalima, M. Kudrjašova, D. G. Kananovich and R. Aav, *ACS Sustain. Chem. Eng.*, 2020, **8**, 15703–15715.
29 D. Langerreiter, M. A. Kostiainen, S. Kaabel and E. Anaya-Plaza, *Angew. Chem., Int. Ed.*, 2022, **61**, e202209033.
30 R. Gujjarappa, R. Khurana, N. Fridman, E. Keinan and O. Reany, *Cell Rep. Phys. Sci.*, 2024, 102011.
31 E. Suut-Tuule, T. Jarg, P. Tikker, K.-M. Lootus, J. Martõnova, R. Reitalu, L. Ustrnul, J. S. Ward, V. Rjabovs, K. Shubin, J. V. Nallaparaju, M. Vendelin, S. Preis, M. Öeren, K. Rissanen, D. Kananovich and R. Aav, *Cell Rep. Phys. Sci.*, 2024, 102161.
32 C. J. Taylor, A. Pomberger, K. C. Felton, R. Grainger, M. Barecka, T. W. Chamberlain, R. A. Bourne, C. N. Johnson and A. A. Lapkin, *Chem. Rev.*, 2023, **123**, 3089–3126.
33 A. Slattery, Z. Wen, P. Tenblad, J. Sanjosé-Orduna, D. Pintossi, T. den Hartog and T. Noël, *Science*, 2024, **383**, eadj1817.
34 S. Lukin, L. S. Germann, T. Friščić and I. Halasz, *Acc. Chem. Res.*, 2022, **55**, 1262–1277.
35 A. A. L. Michalchuk and F. Emmerling, *Angew. Chem., Int. Ed.*, 2022, **61**, e202117270.
36 I. Halasz, S. A. J. Kimber, P. J. Beldon, A. M. Belenguer, F. Adams, V. Honkimäki, R. C. Nightingale,

R. E. Dinnebier and T. Friščić, *Nat. Protoc.*, 2013, **8**, 1718–1729.
37 D. Gracin, V. Štrukil, T. Friščić, I. Halasz and K. Užarević, *Angew. Chem., Int. Ed.*, 2014, **53**, 6193–6197.
38 P. F. M. de Oliveira, A. A. L. Michalchuk, A. G. Buzanich, R. Bienert, R. M. Torresi, P. H. C. Camargo and F. Emmerling, *Chem. Commun.*, 2020, **56**, 10329–10332.
39 J. G. Schiffmann, F. Emmerling, I. C. B. Martins and L. Van Wüllen, *Solid State Nucl. Magn. Reson.*, 2020, **109**, 101687.
40 E. Bartalucci, C. Schumacher, L. Hendrickx, F. Puccetti, I. d'Anciães Almeida Silva, R. Dervişoğlu, R. Puttreddy, C. Bolm and T. Wiegand, *Chem.–Eur. J.*, 2023, **29**, e202203466.
41 I. Halasz, T. Friščić, S. A. J. Kimber, K. Užarević, A. Puškarić, C. Mottillo, P. Julien, V. Štrukil, V. Honkimäki and R. E. Dinnebier, *Faraday Discuss.*, 2014, **170**, 203–221.
42 D. Langerreiter, M. A. Kostiainen, S. Kaabel and E. Anaya-Plaza, *Angew. Chem., Int. Ed.*, 2022, **61**, e20220903.
43 S. Mahajan and I. P. Singh, *Magn. Reson. Chem.*, 2013, **51**, 76–81.
44 R. Muhamadejev, R. Melngaile, P. Paegle, I. Zibarte, M. Petrova, K. Jaudzems and J. Veliks, *J. Org. Chem.*, 2021, **86**, 3890–3896.
45 N. N. Andersen, M. Lisbjerg, K. Eriksen and M. Pittelkow, *Isr. J. Chem.*, 2018, **58**, 435–448.
46 R. Aav, E. Shmatova, I. Reile, M. Borissova and F. Topić, *Org. Lett.*, 2013, **15**, 3786–3789.
47 E. Prigorchenko, M. Öeren, S. Kaabel, M. Fomitšenko, I. Reile, I. Järving, T. Tamm, F. Topić, K. Rissanen and R. Aav, *Chem. Commun.*, 2015, **51**, 10921–10924.
48 S. Kaabel and R. Aav, *Isr. J. Chem.*, 2018, **58**, 296–313.
49 T. Friščić, S. L. Childs, S. A. A. Rizvi and W. Jones, *CrystEngComm*, 2009, **11**, 418–426.
50 M. Fomitšenko, A. Peterson, I. Reile, H. Cong, S. Kaabel, E. Prigorchenko, I. Järving and R. Aav, *New J. Chem.*, 2017, **41**, 2490–2497.
51 M. Lisbjerg, H. Valkenier, B. M. Jessen, H. Al-Kerdi, A. P. Davis and M. Pittelkow, *J. Am. Chem. Soc.*, 2015, **137**, 4948–4951.